Blind Separation of Component Information from Mixed Pixels in Hyperspectral Imagery

Tao Xin, Fan Wenjie, Xu Xiru
Institute of Remote Sensing and Geographic Information System
Peking University
Beijing, China
taoxin@pku.edu.cn

***Abstract*—Mixed pixel separation has always been a hotspot issue of quantitative remote sensing and is especially important for hyperspectral imagery. A new method based on independent component analysis is proposed in this paper to blind separate component information including the signature and the weight from the spectrum of mixed pixels. The extra information is obtained from the statistical characters of the signatures. To evaluate the performance of the algorithm some computer numerical simulations are conducted and a method to choose a best band coverage of the spectrum using for blind signal separation is proposed. Finally the algorithm is applied on the HYPERION imagery of Henshan, Shanxi Provience and the result showed that the method is effective.**

Keywords- Blind signal separation (BSS); Independent Component; mixed pixel; hyperspectral

I. INTRODUCTION

The obstacle to precisely getting the ground information from remote sensing images is the widely existing mixed pixels [1]. Unfortunately, due to the high spectral resolution and the relatively low spatial resolution of hyperspectral imaging sensors, most hyperspectral pixel is possible to be mixed by several substances [2]. So it becomes so useful to do the mixed spectral separation that more ground information can be gained from the hyperspectral data, which is also a difficulty in the field of hyperspectral remote sensing. This paper focuses on solving the problem by introducing a new method called independent component analysis based blind signal separation algorithm (ICA-BSS).

ICA-BSS is based on the linear spectral mixing model that the signature matrix of the pixels can be expressed by the product of the weight matrix and the signature matrix of the components. Its purpose is to simultaneously get the two matrixes while only the signatures of the pixels are given, which is accomplished by using the statistical character of the signatures [3-6].

The main contents of this paper are as follows. Section 2 introduces the idea of the proposed ICA-BSS approach. Section 3 conducts computer simulations to validate the algorithm. Section 4 applies the algorithm on real hyperspectral imagery. Finally, section 5 concludes some remarks.

II. BLIND SIGNAL SEPARATION BASED ON INDEPENDENT COMPONENT ANALYSIS (ICA-BSS)

Suppose the band number of the hyperspectral data is M, the number of the components is N and the number of the mixed pixels is J ($J \geq N$). For simplicity, we further suppose that $J=N$ or this can be achieved by principle component analysis (PCA). Suppose the spectral information of the pixels is expressed by the matrix $\boldsymbol{X}_{N\times M}$, of which the data in a row is the spectrum signature data of a pixel; $\boldsymbol{A}_{N\times N}$ is the component proportion matrix of the pixels, of which the data in a row is the proportions of the N components in a pixel; and $\boldsymbol{S}_{N\times M} = (\boldsymbol{s}_1, \boldsymbol{s}_2, \cdots, \boldsymbol{s}_N)^T$ is the signature matrix of the components, of which the data in a row is the spectrum signature data of a component. If the signatures of the N pixels are linearly mixed by the signature of N components, we have the equation as follows:

$$\boldsymbol{X}_{N\times M} = \boldsymbol{A}_{N\times N}\boldsymbol{S}_{N\times M} \tag{1}$$

If the matrix $\boldsymbol{X}$ is linear transformed by $\boldsymbol{W}$, further supposing $\boldsymbol{W} = \boldsymbol{A}^{-1}$, then the resulting matrix $\boldsymbol{WX}$ is actually the component signature matrix $\boldsymbol{S}$. Thus, the main task of BSS is to find the required $\boldsymbol{W}$, which is accomplished by making use of the statistical character of the linear transformed matrix $\boldsymbol{WX}$.

The Central Limit Theorem tells that the distribution of a sum of independent random variables tends forward a Gaussian distribution under certain conditions. Thus, the row vectors of $\boldsymbol{X}$ usually have distributions that are closer to Gaussian than those of $\boldsymbol{S}$. Denote the linear transformed matrix by $\boldsymbol{Y} = \boldsymbol{WX} = \boldsymbol{WAS}$, let $\boldsymbol{Z} = \boldsymbol{WA}$, then $\boldsymbol{Y} = \boldsymbol{ZS}$, which means that each row vector $\boldsymbol{y}_i$ of $\boldsymbol{Y}$ is a linear combination of the row vectors $\boldsymbol{s}_i$ of $\boldsymbol{S}$ with weights given by z_i. Since a linear combination of $\boldsymbol{S}$ is more Gaussian than $\boldsymbol{S}$, $\boldsymbol{y}_i$ is more Gaussian than any of the $\boldsymbol{s}_i$, and becomes least Gaussian when it in fact equals one of the $\boldsymbol{s}_i$. Therefore, the required $\boldsymbol{W}$ is taken when it maximizes the non-Gaussianity of the linear trans-formed matrix $\boldsymbol{Y}$ [4].

The non-Gaussianity of the probability density function (pdf) of a random variable could be described by kurtosis or negentropy. The kurtosis of a random variable y is defined by

National Natural Science Foundation of China, No. 40401036
Major State Basic Research Development Program of China, No. 2000077900

$kurt(y) = E\{y^4\} - 3\left(E\{y^2\}\right)^2$ where E represents the expectation; *kurt* = 0 for Gaussian pdf, *kurt* > 0 for super-Gaussian pdf, *kurt* < 0 for sub-Gaussian pdf. The negentropy of y is defined by $J(y) = H(y_{gauss}) - H(y)$ where y_{gauss} is a Gaussian random variable of the same variance as y and H represents the entropy $H(y) = -\int f(y)\log f(y)dy$; the fundament for negentropy is that a Gaussian variable has the largest entropy among all random variables of equal variance.

The fast fixed-point algorithm using negentropy is chosen to implement BSS. The algorithm is as follows [5]:

1. Center and whiten the matrix $\boldsymbol{X}$
2. Randomly choose an initial mixing matrix $\boldsymbol{W}$ and orthogonalize it as in step 4.
3. For every $i = 1,...,N$, let $\boldsymbol{w}_i^+ = E\{\boldsymbol{X}g(\boldsymbol{w}_i^T\boldsymbol{X})\} - E\{g'(\boldsymbol{w}_i^T\boldsymbol{X})\}\boldsymbol{w}_i$
4. Do a symmetric orthogonalization of the matrix $\boldsymbol{W}^+$ by $\boldsymbol{W} = \left(\boldsymbol{W}^+\boldsymbol{W}^{+T}\right)^{-1/2}\boldsymbol{W}^+$
5. If not converged, go back to step 3

The function g commonly has two forms: $g_1(u) = \tanh(au)$, where $1 \le a \le 2$ is some suitable constant; $g_2(u) = u\exp(-u^2/2)$. Here we choose g_2 to do the later work.

Several preconditions are needed to make sure the algorithm run well: (1) the signature of the pixels is linearly mixed by the signature of the components and the matrix $\boldsymbol{A}$ is constant, (2) the components must be statistically independent, (3) the probability density functions (pdf) of the component signatures must be non-Gaussian, at most one signature of the components is Gaussian.

It is important to note that due to the property of neg-entropy that it is scale-invariant, i.e., multiplication of a random variable by a constant does not change its negentropy, if $\boldsymbol{W}$ is a solution, $\boldsymbol{\Lambda W}$ is also a solution where $\boldsymbol{\Lambda}$ is a constant diagonal matrix, which means that the amplitude of the component signature is uncertain if only the negentropy information is used. Fortunately, by adding the constraint that the sum of each row in $\boldsymbol{A} = \left(\boldsymbol{W}^*\right)^{-1} = \left(\boldsymbol{\Lambda}^*\boldsymbol{W}\right)^{-1}$ (where $\boldsymbol{W}^*$ is the actual solution) must equal to unity, the problem can be easily solved. In more details, it is done by first expressing the matrix $\left(\boldsymbol{\Lambda W}\right)^{-1}$ as:

$$(\boldsymbol{\Lambda W})^{-1} = \boldsymbol{W}^{-1}\boldsymbol{\Lambda}^{-1} = \begin{bmatrix} c_{11} & \cdots & c_{1N} \\ \vdots & \ddots & \vdots \\ c_{N1} & \cdots & c_{NN} \end{bmatrix}\begin{bmatrix} \Lambda_{11}^{-1} & & \\ & \ddots & \\ & & \Lambda_{NN}^{-1} \end{bmatrix} = \begin{bmatrix} c_{11}\Lambda_{11}^{-1} & \cdots & c_{1N}\Lambda_{NN}^{-1} \\ \vdots & \ddots & \vdots \\ c_{N1}\Lambda_{11}^{-1} & \cdots & c_{NN}\Lambda_{NN}^{-1} \end{bmatrix} \quad (2)$$

where $c_{ij}(i, j = 1,\ldots,N)$ is the element of $\boldsymbol{W}^{-1}$ and then solving the equations $c_{11}\Lambda_{11}^{-1} + \cdots + c_{1N}\Lambda_{NN}^{-1} = 1, \ldots, c_{N1}\Lambda_{11}^{-1} + \cdots + c_{NN}\Lambda_{NN}^{-1} = 1$ for $\Lambda_{11}^*, \ldots, \Lambda_{NN}^*$.

III. THE COMPUTER NUMERICAL SIMULATION

In order to quantitatively evaluate the effectiveness of ICA-based blind signal separation, some computer numerical simulations are conducted in this section to separate two or more components from the hyperspectral data. The spectral data of grass, soil, some minerals and water for the experiment is obtained from the spectral library of ENVI. The band coverage of the spectral signatures is chosen from 0.4μm to 2.56μm and the spectral data is interpolated with a step size of 0.001μm.

A. Separation of two components

The spectral signatures of grass and soil are used in the simulation of two components. Suppose one mixed pixel is composed of 20% of grass and 80% of soil and the other is composed of 90% of grass and 10% of soil, the signatures of them are shown in Fig. 1.

After the signatures of two pixels are simulated, ICA-BSS is performed on them to get the signatures of the components and their corresponding proportions in the two pixels. Comparisons of the retrieved signatures and the original signatures are shown in Fig. 2 and comparisons of the retrieved proportions and the actual proportions are shown in table I.

As shown in Fig. 2, the two curves of the retrieved signatures are nearly the same as the original curves. Table I shows that the error of the component proportions retrieved is less than 2% of the pixel area. Further experiments show that when the original proportion of the components are changed, the retrieved signatures remain almost the same and the errors of the component proportions retrieved maintain small, concluding that the component proportion has little effect on the separating result.

It is worth noting that the band coverage of this BSS experiment is 0.59-2.28μm (different from the band coverage chosen from the spectral library (0.4-2.56μm)), as better results could be obtained by adjusting the band coverage used. Some experiments were done to investigate a best band coverage. In each experiment different band coverage was chosen and the kurtosis of the signatures of the two components was also calculated. We discover some relationship between the inversion error and the difference of the kurtosis of the two component signatures, which was depicted in Fig. 3.

As shown in Fig. 3, when the difference is large enough, the error is low and could be restricted within an extent; additionally, experiment data also show that in most of such cases, one kurtosis is positive and the other negative and their values are far from zero. However, when the kurtosis between the two component signatures has little difference, it becomes difficult for the algorithm to precisely recover the two components, and sometimes the inversion error could be very high. Thus we figure out from these experiments a method for choosing a best band coverage is to maximize the non-Gaussianity of the signature of the components in the chosen spectral coverage and the non-Gaussianity at best to be different (one is super-Gaussian, and the other sub-Gaussian).

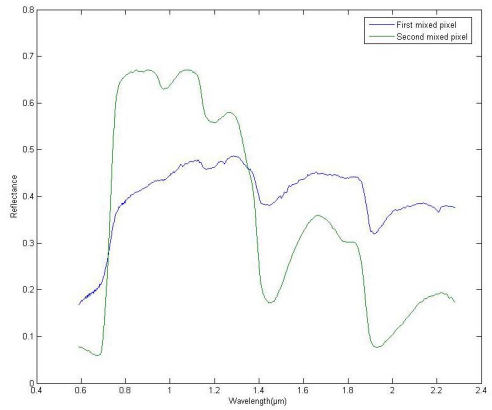

Figure 1. The spectral curve of two mixed pixels (the first pixel is composed of 20% of grass and 80% of soil; the second pixel is composed of 90% of grass and 10% of soil).

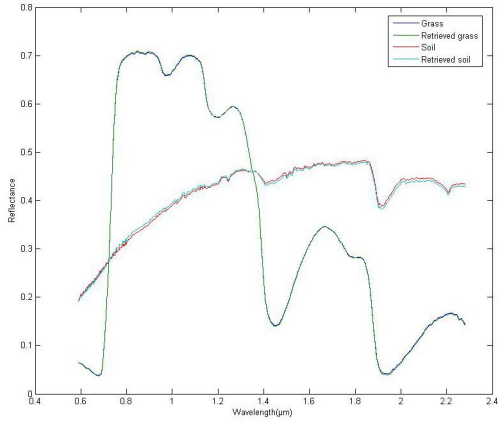

Figure 2. Comparisons of the retrieved signatures and the original signatures.

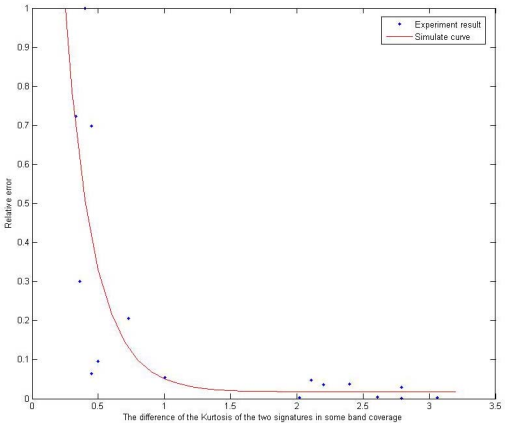

Figure 3. The relationship between the relative error and the difference of the kurtosis of the two signatures.

The ICA-BSS method is based on the statistical character of the data and thus the sample number may have some effects on the experiment error. The relationship between the variance of the recovered and original signatures of the components and the band number is shown in Fig. 4.

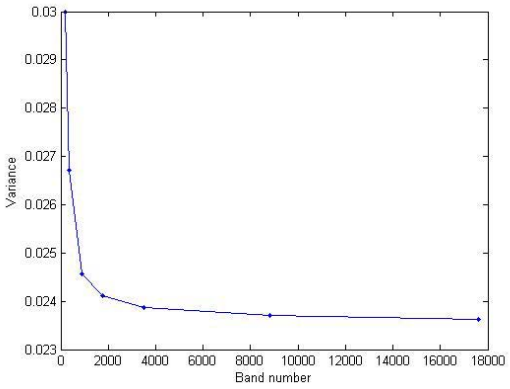

Figure 4. The relationship between the variance of the recovered and original signatures of the components and the band number

TABLE I. THE RETRIEVED RESULT OF COMPONENT PROPORTIONS BY ICA-BSS, COMPARED WITH ORIGINAL DATA.

Component proportion (%)	**Pixel I**		**Pixel II**	
	Original	***Retrieved***	***Original***	***Retrieved***
Grass	20	18.5	90	89.3
Soil	80	81.5	10	10.7

As shown in Fig. 4, as the band number increases from a small value, the variance decreases sharply in the beginning, gradually slows down the rate and eventually approaches a constant.

To know the error sensitivity of the fast fixed-point algorithm using negentropy, random errors of 5%, 10% and 20% are added to the signature matrix of pixels. Table II shows the result of ICA-BSS. It is obvious that the method of BSS is not sensitive with errors; Even if 20% input errors are added, the inversion error can also be restricted within 10%. As a result of the influences of random noises, the inversion curves are filled with random high frequency fluctuations; the inversion results are obviously improved filtering by B-Spline function [1].

B. Separation of more than two components

The spectral signatures of grass, soil, water and some minerals are used in the simulation of ICA-BSS of N (N≥3) components. Experiment results show the algorithm also effective in such cases. Due to the coherence among the signatures of some components, the inversion error augments

TABLE II. THE INVERSION RESULT OF THE COMPONENT SIGNATURES WHEN ERRORS ARE ADDED (Σ REPRESENTS STANDARD DEVIATION).

Error(%)	**100 * Grass signature**				**100 * Soil signature**			
	Maximum	***Minimum***	***Average***	***σ***	***Maximum***	***Minimum***	***Average***	***σ***
5	5.1092	0.0006	1.6997	0.037	3.614	0	0.83	0.011
10	8.483	0.002	2.0573	0.063	6.389	0	1.6047	0.04
20	15.727	0.002	3.9966	0.245	17.424	0.002	4.0094	0.253

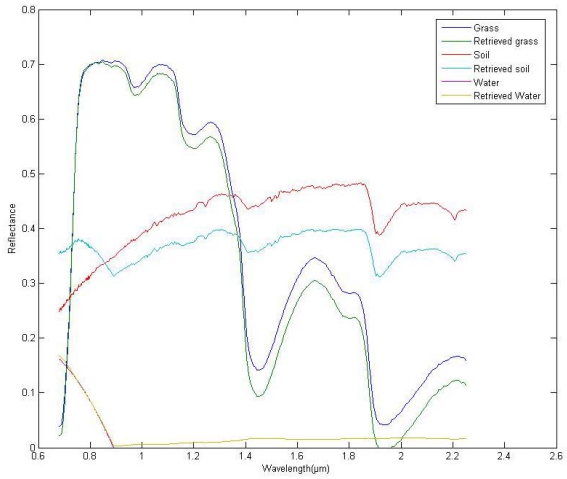

Figure 5. The inversion result when the mixed pixels are composed of grass, soil and water.

as the components increases but is still tolerable. Fig. 5 shows the inversion result when the mixed pixels are composed of grass, soil and water.

IV. FIELD VALIDATIONS

It is used in this experiment the HYPERION imagery of the distinct in Shanxi Province (37.7-37.9°N，109.1-109.3°E) on July 7, 2005 to compute the compositions of the pixels by the ICA-BSS method and the SPOT5 imagery of the same distinct at the same period is used to validate the result. The spatial resolution of HYPERION is 30m and that of SPOT5 is 10m.

After doing corrections to the two imageries so that each pixel in HYPERION imagery corresponds to 3*3 pixels in SPOT5 imagery, choose an area of 10*10 pixels from the HYPERION imagery processed and run the algorithm of two components to each pair of two pixels. Therefore each pixel has to do 99 times of BSS and the result is averaged. The result of vegetation proportions in all pixels is shown in Fig. 5(a).

To validate the result of HYPERION, we also calculate the proportion of vegetation in each of the 10*10 pixels by using the SPOT5 imagery data. The result of SPOT5 is shown in Fig. 5(b).

The result shows that the vegetation and soil proportion inversed by BSS is close to the result of the SPOT5 imagery. The errors are due to the following reasons: (a) the error caused by the process of geometry correction; (b) the components in some pixels are quite different from those in other pixels. The latter causes the invalidation of the algorithm of two components on these pixels.

V. CONCLUSIONS

This paper presents an ICA-based BSS algorithm to separate component information including their spectrum and proportions in the mixed pixels from hyperspectral imagery

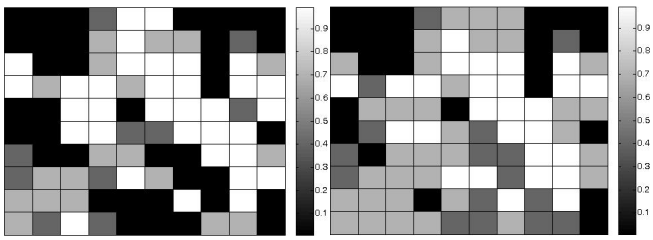

(a) (b)

Figure 6. The proportion of vegetation inversed by ICA-BSS in HYPERION image (a).For comparison, the proportion of vegetation in SPOT5 image (b).

data. The simulation shows that this method is robust and can be effectively implied on real hyperspectral imagery. The real-hyperspectral-image experiment demonstrates that the result by BSS is close to the result obtained from an imagery of higher resolution. However the relative error for the experiment is about 20%, which is difficult to satisfy the request of pplication. It is not only because of the error caused by the process of corrections, but also due to the problem existing in the BSS method itself. The accuracy of the method is affected when the components in some pixels are inhomogeneous. Therefore the algorithm needs further improving to reduce the error.

ACKNOWLEDGMENT

Authors would like to thank Prof. A. Hyvarinen for providing the ICA code [5] and Dr. Liu Qiang for helpful suggestions.

REFERENCES

[1] Fan W. J. , & Xu X. R. A method for blind separation of components information from mixed pixel. Progress in Natural Science, vol. 16, No.7, pp. 760-765, 2006

[2] Jing Wang & Chein-I Chang. Applications of independent component analysis in endmember extraction and abundance quantification for hyperspectral imagery. Geoscience and Remote Sensing, vol. 44, No. 9, pp. 2601-2616, 2006.

[3] Hyvarinen,A.,&Oja,E. A fast fixed point algorithm for independent component analysis . Neural Comp, vol. 9, pp. 1483-1491, 1997.

[4] Hyvarinen, A. & Oja, E. Independent component analysis: algorithms and applications. Neural Networks, vol. 13, pp. 411-430, 2000.

[5] Hyvarinen, A. Karhumen, J. & Oja, E. Independent component analysis. New York, J. Wiley, 2001.

[6] Comon P. Independent component analysis, a new concept? Signal processing, vol. 36, pp. 287-314, 1994.

[7] Nascimento JMP & Dias JMB. Does independent component analysis play a role in unmixing hyperspectral data? Geoscience and Remote Sensing, vol. 43, No. 1, pp. 175-186, January 2005.

[8] Stone, J V. Independent component analysis: a tutorial introduction. MIT Press, 2004

[9] Xu X.R. Zhou L.F. & Zhu X.H. The factor analysis method of mixed pixel and its application for area estimation sown with winter wheat in large area. Chinese Science Bulletin, vol. 34, No. 12, pp. 946-949, 1989.

[10] Yang Z.Q., Li Y. & Hu D.W. Independent component analysis: a survey. Acta Automatica Sinica, vol. 28, No. 5, pp. 762-772,2002.